

Identification of Functional Model for Piezoelectric Based on Radial Basis Function Network

César A. Hernandez S.¹, Diego A. Giral R.² and Fredy H. Martínez S.^{3*}

¹Full Professor, Facultad Tecnológica, Universidad Distrital Francisco José de Caldas, Colombia.
ORCID: 0000-0001-9409-8341

²Assistant Professor, Facultad Tecnológica, Universidad Distrital Francisco José de Caldas, Colombia.
ORCID: 0000-0001-9983-4555

³Associate Professor, Facultad Tecnológica, Universidad Distrital Francisco José de Caldas, Colombia.
ORCID: 0000-0002-7258-3909

*Corresponding Author

Abstract

This paper studies the development of a functional model of a piezoelectric energy harvester (PEH) as part of the framework for the development of design schemes for energy harvesting systems for the collection of vibration induced by the passage of people in public spaces at medium and large scales. The model is based on the laboratory results of a piezoelectric device coupled with a cowhide material, a configuration of higher performance and economy according to our previous research. We seek to replicate the behavior using a mathematical model based on a radial basis function network, for which a structure is tuned based on the variation of the learning rate, the number of neurons in the hidden layer, and the opening characteristics of the bells in each of the nonlinear activation functions. The search and tuning algorithm was trained using a hybrid setup, in which the centers of the functions and their variances are set in each trial in a non-supervised manner, and then the network weights are adjusted in a gradient supervised manner. The resulting models were compared using a similarity vector concerning the laboratory data, showing that in general the models with varying Gaussian widths and a reasonable number of centers show better performance. These results provide a good basis for the exploration and design of multiple piezoelectric energy harvesting systems.

I. INTRODUCTION

The United Nations (UN) has just issued a warning in its Climate Change 2021 report, in which they raise the crisis related to climate, biodiversity, and pollution. This problem has been analyzed and some countries have tried to reduce it through environmental policies, many of them related to the generation of electric energy, which for many is a strong element of environmental alteration [1, 2, 3, 4, 5]. These policies establish the need to increase the share of renewable resources as well as to develop advanced solutions for electricity generation [6, 7]. Research in this area has taken on a broad spectrum that includes, but is not limited to, the reuse

of biological materials as fuel, optimization of generation systems, and the use of new sources such as piezoelectric materials [8, 9, 10].

Piezoelectric materials work by transforming kinetic energy (ideally all that already exists in the environment) into electrical energy. This kinetic energy from the environment can be taken from systems such as the displacement of fluids, or the movement of organisms such as vehicles, animals, or people, elements already existing in life today, which is why this source of energy is highly clean and is projected to be of great importance, particularly in distributed generation systems [11, 12]. While there are currently electric machine-based schemes for electric power generation, these systems have been designed for large-scale generation, which is environmentally harmful and inefficient for low-power generation. Piezoelectrics can be used with minimal interference in existing kinetic systems, allowing distributed, low-power energy harvesting [13, 14, 15].

The vibrations produced by the activity of bodies such as vehicles, animals, or people are renewable sources of energy because they are resources that are naturally restored over time. They are natural phenomena that although of low power, can be used as energy sources. For example, in the walk of the human being, from the footsteps, it is possible to recover between 5 and 8 W [16, 17]. Energy harvesting from a piezoelectric is quite easy, despite the complexity of the design and layout of piezoelectrics, and their initial cost. The energy collected from a piezoelectric is characterized by being compact, simple, low maintenance, and fast conversion, coupled with the fact of its low power makes it widely used to charge low power devices. Many of the energy solutions with these devices are aimed at supporting other industries where high kinetic energy can be harvested [18, 19].

Such schemes have been widely used in recent years in IoT (Internet of Things) scenarios. For example, research has been documented in which these devices have been integrated into a smart cargo container system, taking advantage of the characteristics of low and intermittent ambient energy, and combining it with a traditional thermal generation system,

which has positively impacted the life of the system's batteries [20]. Other cases of hybrid systems use piezoelectrics in conjunction with other alternative kinetic energy conversion systems, such as magnetic field interaction, resulting in a higher energy yield from the same kinetic energy source [19]. Cases have also been reported in which piezoelectrics are combined with photovoltaic generation systems to simultaneously harvest kinetic wind energy and radiant solar energy, as in the previous case, a hybrid system with higher capacity and efficiency is achieved, with high benefits in low-power distributed generation systems [21, 22]. An interesting case of a piezoelectric scheme considers its use in ultrasonic wireless charging systems, particularly when these systems are carried by individuals, who ultimately produce the kinetic energy with their movement. While these systems prove to be too bulky and rigid to date, flexible schemes with multiple piezoelectrics in several layers capable of producing continuous electrical power outputs have already been proposed [23].

However, the design and projection of the generating capacity of these installations involve the selection of many parameters that are not yet standardized in this technology and depend on the particular operating conditions [24]. For the design of these systems, it is necessary to quantify the power capacity generated according to the device, its layout, and the particular characteristics of use. From this study, it is possible to estimate the energy efficiency of piezoelectrics, and that of the entire generation system in combination with other renewable energy sources in the case of hybrid systems, a topology that is currently being used [15]. The nonlinear behavior of these devices and their dependence on piezoelectric variables and their configuration can be identified by nonlinear learning models such as artificial neural networks (ANN) [25, 26]. With these systems, it is possible to create behavioral models that allow estimating the performance of the system under controlled conditions, before its real implementation. These models are adjusted by learning from behavior observed in the laboratory, so it is always possible to adapt them to the conditions of each implementation [27].

This research seeks to identify such behavior for a particular configuration of piezoelectric, which has been identified for use in the generation of electrical energy from the walking of people in buildings and public spaces by identifying the relationship between generated power and deformation of the material. These tests were developed experimentally through the design of special tiles conditioned with different materials as mechanical support. From the multiple experiments, an average behavior was defined for each case, thus selecting the most convenient configuration for the designs. This paper continues this work by characterizing a functional model of the system that can be used to predict the energy efficiency of power generation in different configurations.

II. PROBLEM FORMULATION

As a strategy for harvesting electrical energy in public facilities, the behavior of piezoelectric ceramic PZT (Lead Zirconate Titanate) against mechanical deformation (walking of people with an average weight of 60 kg) is studied, given its availability and low cost. These devices were studied in the

laboratory under different configurations, which sought to reduce their mechanical degradation while maximizing electrical performance. The coupling of the piezoelectrics was studied with different materials (including wood, Bakelite, PLA, and leather) and in different configurations, which allowed defining an architecture for the strain-transmitting tiles and the coupling material (cowhide). The typical electrical behavior of the selected coupling is shown in Fig. 1.

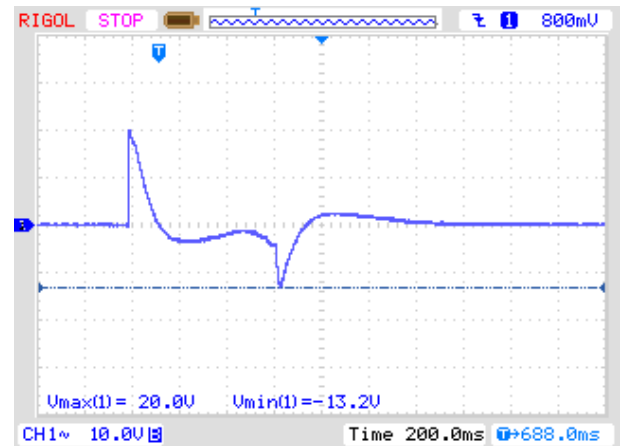


Fig. 1. Laboratory captured curve of piezoelectric behavior under the operating conditions to be identified and replicated

It is proposed to model this electrical behavior using an ANN, in particular using a radial basis function network. This decision is based on the possibility of selecting the number of neurons in the hidden layer of the network from laboratory data (curve topology), which allows the definition of a sub-optimal network architecture for the nonlinear curve that characterizes the piezoelectric activation (Fig. 1). Optimizing the size of the network facilitates the model fitting, and ensures that the network can be adapted to any curve, in case of modifications to the mechanical design.

The network fitting is done in a hybrid way (hidden layer in a non-supervised way according to the behavior of the data, and then output weights in a supervised way), and considers the behavior of various parameters. In particular, different tests are performed by varying both the topology of the radial functions and the learning rate of the gradient descent algorithm.

III. METHODOLOGY

Radial basis function networks correspond to a special type of artificial neural network characterized by defining their output from a set of distance functions to a point called the center. These networks use these radial functions as the activation function. The output of the network corresponds to a linear combination of these radial functions, which include the inputs and the parameters of the neurons. These types of networks form approximations that are linear combinations of multiple local non-linear functions. Fig. 2 shows a schematic representation of a radial basis function network, the inputs are represented by the variables $x_1, x_2, x_3, \dots, x_n$, which constitute the

input vector X . The radial functions are located in each of the neurons of the hidden layer, and the weights to be tuned, $w_1, w_2, w_3, \dots, w_N$, connect the hidden layer with the output linear combiner.

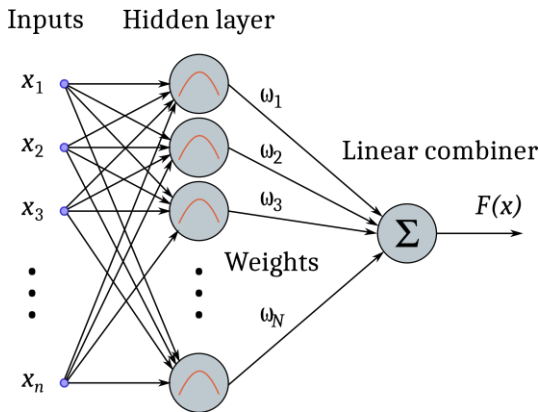


Fig. 2. Radial basis function network with input nodes detail, non-linear hidden layer, and output linear combiner

Like multilayer perceptrons, they serve as universal approximators. However, in the multilayer perceptron, the network is trained by reducing the error (optimization), with radial basis function networks the goal is to approximate the surface to a high-dimensional space. Learning is equivalent to finding a surface in a multidimensional space that provides the best fit to the training data.

Radial basis function (RBF) networks typically have three layers: an input layer, a hidden layer with a non-linear activation function, and a linear output layer. The transformation from the input space to the space of the hidden units is non-linear, and the transformation from the space of the hidden units to the output space is linear. The hidden units are a set of functions that form an arbitrary basis for the input patterns when expanded in the space of the hidden units, these functions are called radial functions. The radial basis function is a function that computes the Euclidean distance of an input vector x to a center c . (Eq. 1).

$$f(x) = \|x - c_i\| \quad (1)$$

To each neuron in the input layer corresponds a radial basis function $\Phi(x)$ and an output weight ω_i . The output of an RBF network is (Eq. 2):

$$F(x) = \sum_{i=1}^N \omega_i \Phi(\|x - c_i\|) \quad (2)$$

Where $\Phi(\|x - c_i\|)$ is a set of N arbitrary functions known as radial functions. The data c_i are the centers of the radial functions. The function $\Phi(\|x - c_i\|) = \Phi(r)$, with r as the Euclidean distance, can be of several types (Eqs. 3-6):

$$\Phi(r) = e^{-(\epsilon r)^2}, \text{ Gaussian function} \quad (3)$$

$$\Phi(r) = \sqrt{1 + (\epsilon r)^2}, \text{ Multiquadratic function} \quad (4)$$

$$\Phi(r) = \frac{1}{\sqrt{1 + (\epsilon r)^2}}, \text{ Inverse multiquadratic function} \quad (5)$$

$$\Phi(r) = r^2 \ln(r), \text{ Thin plate spline function} \quad (6)$$

We use the Gaussian function to fit our model. The ϵ parameter depends on the variance and controls the width of the Gaussian bell.

Learning consists of determining the centers, variances, and weights from the hidden layer to the output layer. As the network layers perform different tasks, the parameters of the hidden layer will be separated from the output layer to optimize the process. In this way, the centers and variances follow a process guided by an optimization in the input space, while the weights follow an optimization based on the desired outputs.

There are two learning strategies, the hybrid method (centers and variances determined in a non-supervised way, and then the calculation of weights in a supervised way) and the fully supervised method (or integrated method, which tries to minimize the mean square error using the gradient). In our research we have used a hybrid method with the following characteristics:

- In the unsupervised phase, the centers and deviations of the radial basis functions are determined to group the input space into different classes or categories.
- The representative of each class will be the center of the radial basis function, and the deviation will be given by the amplitude of each class.
- An unsupervised classification algorithm (k -means clustering) is used to divide the input space into classes or clusters. In this sense, tests are performed for different values of k to observe the behavior concerning this variable.
- The number of clusters will be the number of hidden neurons in the radial basis network.
- To determine the deviations, the amplitudes are calculated such that each hidden neuron is activated in the region of the input space, and such that the overlap of the activation zones from one neuron to another is as slight as possible. To evaluate the sensitivity to this parameter, tests are performed with variable amplitudes according to the data and fixed or constant amplitudes.
- In the supervised phase, the weights and thresholds of the output layer are determined in a supervised manner.

The behavioral characteristic curve (Fig. 1) was sampled at a rate of 21.3 ms, thus generating a dataset of 75 samples over a total interval of 1.6 s. The fit in all cases was performed for the same dataset.

IV. RESULTS AND DISCUSSION

The results of the model fitting process are shown in Figs. 3 to 6. The blue dots correspond to the laboratory data and the green curve to the fitted model.

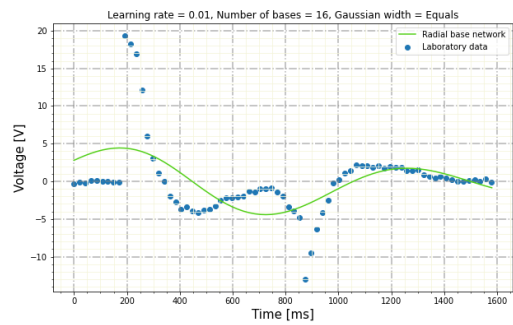
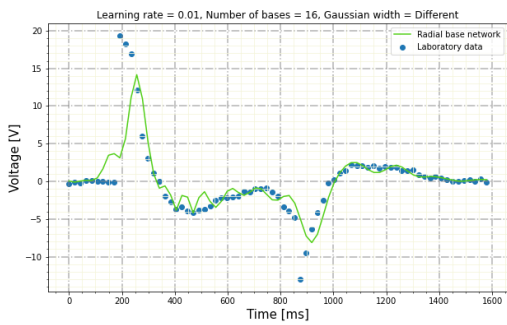
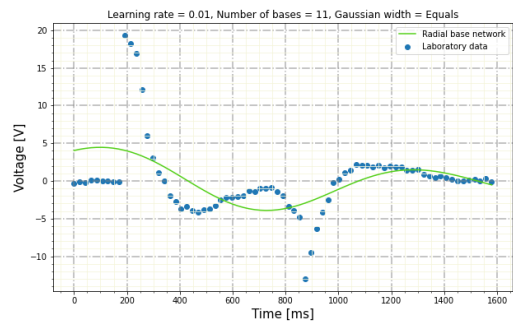
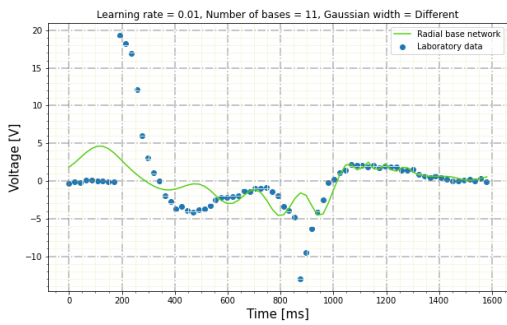
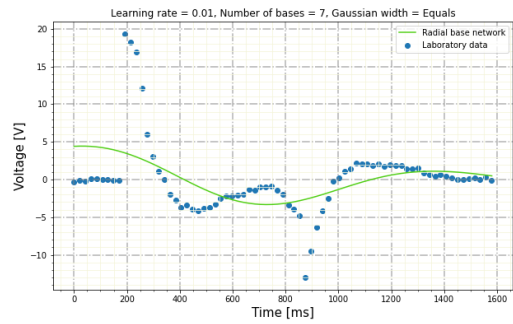
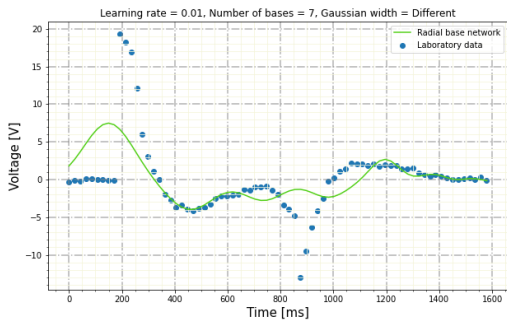
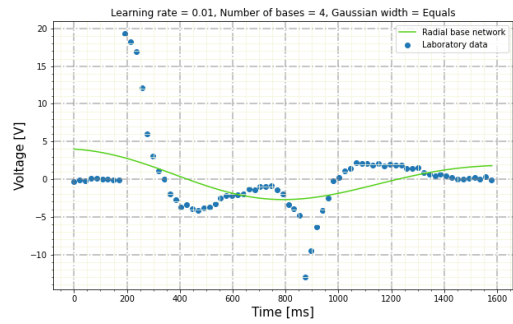
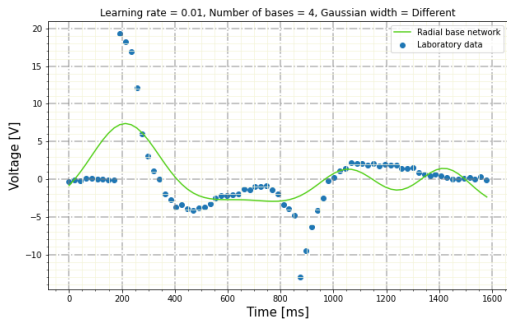
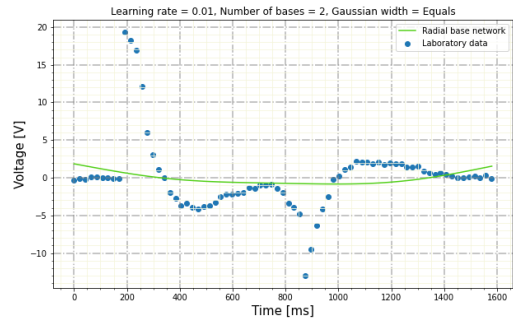
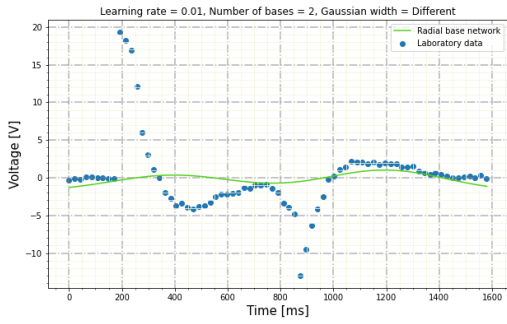


Fig. 3. Learning rate of 0.01, and varying Gaussian widths

Fig. 4. Learning rate of 0.01, and fixed Gaussian widths

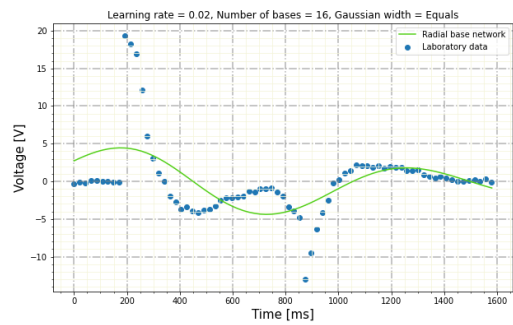
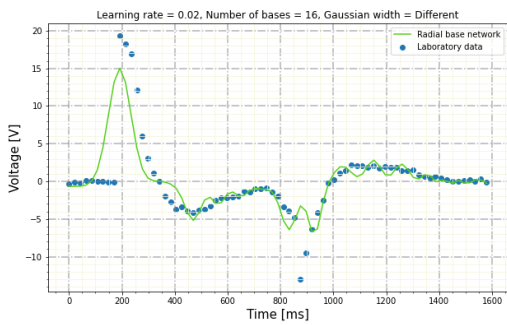
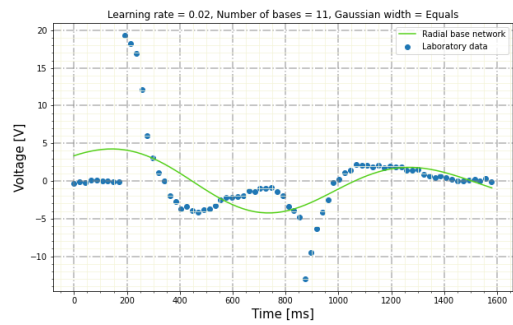
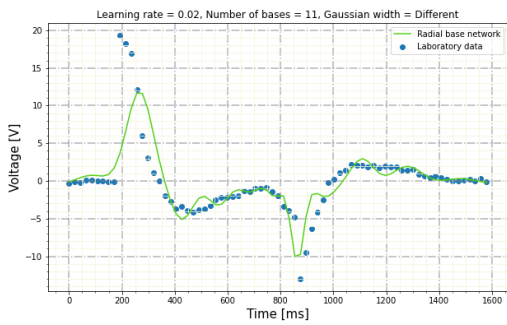
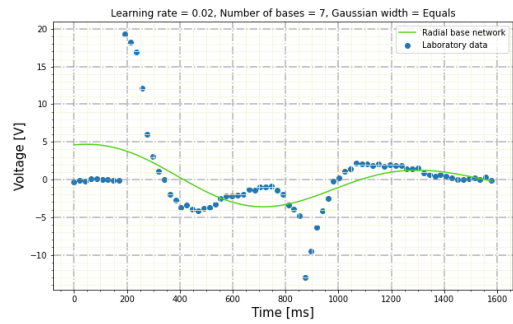
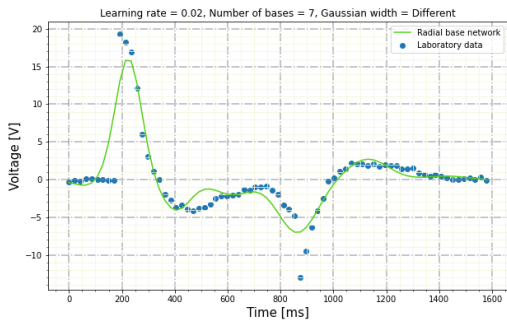
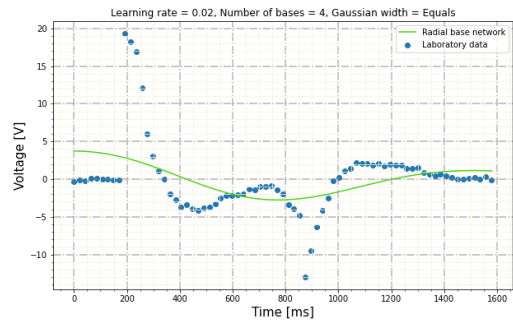
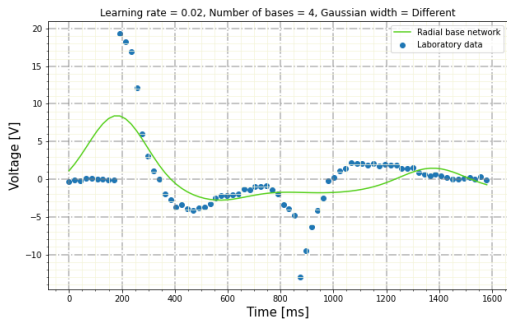
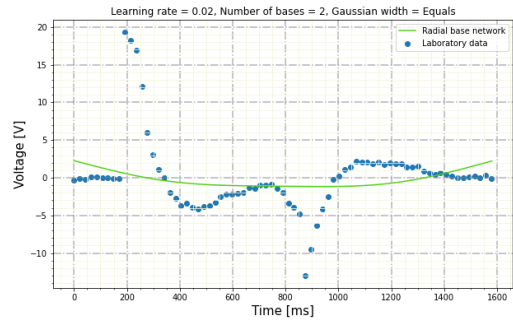
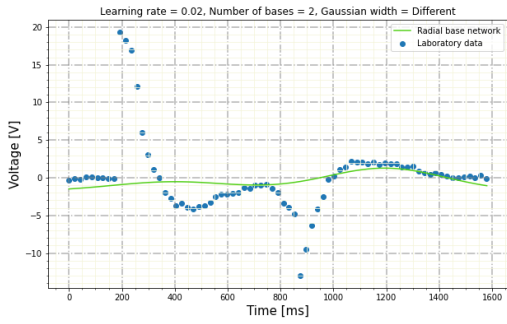


Fig. 5. Learning rate of 0.02, and varying Gaussian widths

Fig. 6. Learning rate of 0.02, and fixed Gaussian widths

The model fit tests were separated into two groups according to the supervised fitting scheme of the linear combiner weights. The first group (Figs. 3 and 4) corresponds to fits using a constant learning rate of 0.01, and the second group (Figs. 5 and 6) used a constant learning rate of 0.02. The objective of this separation was to identify possible benefits in the models about this variable given the hybrid fitting scheme used. In each of the two cases, different tests were performed by altering the parameters of the radial functions of the hidden layer. In particular, the two groups were fitted with 2, 4, 7, 11, and 16 radial functions, and these radial functions were constructed in two ways, both with different Gaussian apertures according to the dispersion of the data, and with fixed Gaussian apertures.

The laboratory data correspond to sampling at 21.3 ms applied to the average behavior measured in the laboratory. For the definition of the centers of the radial functions, we used the k -means clustering algorithm with five different values of k (2, 4, 7, 11, and 16). In each case (each model with a given value of k) we calculated the dispersion of the data around the centroids identified by k -means clustering and defined the opening of the Gaussian bells (both variable and fixed) seeking to reduce the overlap of the functions as much as possible.

Analyzing the results, it is evident that the models using different Gaussian bell widths perform better than the models using fixed bell widths. The bell widths were defined according to the dispersion of the data in each cluster, therefore, each radial function in these models can better identify the data near its center. In the case of fixed bell widths, the uniformity of the radii is not sufficient to adequately represent the nearby data.

Concerning the number of bases or radial functions, very few bases (cases with only 2 or 4 bases) turn out to be insufficient to represent all the data, which was expected according to the behavior of the system. The performance improves considerably when there are seven or more radial functions, especially for models with different Gaussian bell widths. However, when having too many radial functions (16 in our tests) the model tries to replicate the behavior of the data reducing its generalization capability, which reduces the model performance. Finally, the learning rate of 0.02 produces better fits to the linear combiner weights than those obtained with lower values. The best performing model used a learning rate of 0.02, seven bases or radial functions, and adjusted (variable) bell width for each of them.

V. CONCLUSION

This paper presents the adjustment of a functional model of the electrical behavior of a PZT piezoelectric based on a radial basis function network, with the objective of its use in the projection and design of energy harvesting systems in public spaces. According to previous research with this type of piezoelectrics, a mechanical architecture has been defined that maximizes their electrical performance and reduces their wear. With this architecture, laboratory tests were performed to identify its behavior according to the physical layout in a real application. These data were averaged to produce the behavior to be modeled. The tuning of the model considered these data and started from a network structure supported by a hidden

layer of radial functions and an output combiner. As for tuning parameters, both the number of functions in the hidden layer and the Gaussian bell characteristic of each of them were varied. The value of the learning rate was also varied considering that the training of the models was performed in a hybrid way, that is, the radial functions in an unsupervised way, and then the output layer in a supervised way. The location of the centers of the radial functions was defined from the data using the k -means clustering algorithm. The results show a better performance of the model if we use Gaussian bell widths adjusted for each radial function according to the dispersion of the data in each cluster. Better performance is also observed with slightly higher learning rates. In the case of the number of radial functions in the hidden layer, an over-fitting of the network is observed when there are many functions in the model. The sup-optimal value found for the model suggests seven radial functions. This research continues with the modification of the constants of this initial model based on the physical parameters of the mechanical assembly.

ACKNOWLEDGMENTS

This work was supported by the Universidad Distrital Francisco José de Caldas, specifically by the Technological Faculty. The views expressed in this paper are not necessarily endorsed by Universidad Distrital. The authors thank all the students and researchers of the research group ARMOS for their support in the development of this work.

REFERENCES

- [1] C. Sarasa and K. Turner, "Can a combination of efficiency initiatives give us "good" rebound effects?", *Energy*, vol. 235, 2021, ISSN 0360-5442, doi:10.1016/j.energy.2021.121335.
- [2] B. Dey, B. Bhattacharyya, and F. Márquez, "A hybrid optimization-based approach to solve environment constrained economic dispatch problem on microgrid system", *Journal of Cleaner Production*, vol. 307, 2021, ISSN 0959-6526, doi:10.1016/j.jclepro.2021.127196.
- [3] S. Zarei, O. Bozorg-Haddad, S. Kheirinejad, and H. Loáiciga, "Environmental sustainability: A review of the water-energy-food nexus", *Aqua Water Infrastructure, Ecosystems and Society*, vol. 70, no. 2, pp. 138–154, 2021, ISSN 2709-8028, doi:10.2166/aqua.2020.058.
- [4] D. Romero, B. Castellanos, and N. Garzón, "Conserving water is conserving your life", *Tekhnê*, vol. 16, no. 1, pp. 23–34, 2019, ISSN 1692-8407.
- [5] W. Sánchez and V. Guerrero, "Ecology, construction, and innovation: An alert towards change", *Tekhnê*, vol. 15, no. 2, pp. 45–58, 2018, ISSN 1692-8407.
- [6] X. Yang, S. Liu, L. Zhang, J. Su, and T. Ye, "Design and analysis of a renewable energy power system for shale oil exploitation using hierarchical optimization", *Energy*, vol. 206, 2020, ISSN 0360-5442, doi:10.1016/j.energy.2020.118078.

- [7] M. Shahbaz, C. Raghutla, K. Chittedi, Z. Jiao, and X. Vo, "The effect of renewable energy consumption on economic growth: Evidence from the renewable energy country attractive index", *Energy*, vol. 207, 2020, ISSN 0360-5442, doi:10.1016/j.energy.2020.118162.
- [8] M. El Bouti and M. Allouch, "Analysis of Human Factors for Enhancing Safety and Security Management System in Fossil and Renewable Power Plants", *International Journal of Safety and Security Engineering*, vol. 10, no. 4, pp. 491–500, 2020, ISSN 2041-9031, doi:10.18280/ijss.100408.
- [9] A. Khan and N. Javaid, "Jaya Learning-Based Optimization for Optimal Sizing of Stand-Alone Photovoltaic, Wind Turbine, and Battery Systems", *Engineering*, vol. 6, no. 7, pp. 812–826, 2020, ISSN 2095-8099, doi:10.1016/j.eng.2020.06.004.
- [10] M. Deore, "Development of microbial fuel cell as a contribution to renewable energy sources", *International Journal of Engineering and Advanced Technology*, vol. 8, no. 6, pp. 5391–5393, 2019, ISSN 2249-8958, doi:10.35940/ijeat.F8541.088619.
- [11] H.-E. Lange, R. Bader, and D. Kluess, "Design study on customised piezoelectric elements for energy harvesting in total hip replacements", *Energies*, vol. 14, no. 12, 2021, ISSN 1996-1073, doi:10.3390/en14123480.
- [12] J. Patrick, S. Adhikari, and M. Hussein, "Brillouin-zone characterization of piezoelectric material intrinsic energy-harvesting availability", *Smart Materials and Structures*, vol. 30, no. 8, 2021, ISSN 0964-1726, doi:10.1088/1361-665X/ac0c2c.
- [13] Y. Kuang, Z. Chew, J. Dunville, J. Sibson, and M. Zhu, "Strongly coupled piezoelectric energy harvesters: Optimised design with over 100 mW power, high durability and robustness for self-powered condition monitoring", *Energy Conversion and Management*, vol. 237, 2021, ISSN 0196-8904, doi:10.1016/j.enconman.2021.114129.
- [14] M. Sheeraz, M. Malik, K. Rehman, H. Elahi, Z. Butt, I. Ahmad, M. Eugeni, and P. Gaudenzi, "Numerical assessment and parametric optimization of a piezoelectric wind energy harvester for IoT-based applications", *Energies*, vol. 14, no. 9, 2021, ISSN 1996-1073, doi:10.3390/en14092498.
- [15] H. Han and J. Ko, "Power-generation optimization based on piezoelectric ceramic deformation for energy harvesting application with renewable energy", *Energies*, vol. 14, no. 8, 2021, ISSN 1996-1073, doi:10.3390/en14082171.
- [16] A. Gaur, S. Tiwari, C. Kumar, and P. Maiti, "A bio-based piezoelectric nanogenerator for mechanical energy harvesting using nanohybrid of poly(vinylidene fluoride)", *Nanoscale Advances*, vol. 1, no. 8, pp. 3200–3211, 2019, ISSN 2516-0230, doi:10.1039/c9na00214f.
- [17] K. Li, Q. He, J. Wang, Z. Zhou, and X. Li, "Wearable energy harvesters generating electricity from low-frequency human limb movement", *Microsystems and Nanoengineering*, vol. 4, no. 1, 2018, ISSN 2055-7434, doi:10.1038/s41378-018-0024-3.
- [18] T. Jintanawan, G. Phanomchoeng, S. Suwankawin, P. Kreepoke, P. Chetchatree, and C. U-Viengchai, "Design of kinetic-energy harvesting floors", *Energies*, vol. 13, no. 20, 2020, ISSN 1996-1073, doi:10.3390/en13205419.
- [19] S. Chamarian, B. Ciftci, H. Ulsan, A. Muhtaroglu, and H. Kulah, "Power-Efficient Hybrid Energy Harvesting System for Harnessing Ambient Vibrations", *IEEE Transactions on Circuits and Systems I: Regular Papers*, vol. 66, no. 7, pp. 2784–2793, 2019, ISSN 1549-8328, doi:10.1109/TCSI.2019.2900574.
- [20] A. Lopez-Martin, J. Algueta, and I. Matías, "Energy harvesting approaches in IoT scenarios with very low ambient energy", *Renewable Energy and Power Quality Journal*, vol. 17, pp. 183–187, 2019, ISSN 2172-038X, doi:10.24084/repqj17.257.
- [21] A. Cioncolini, M. Nabawy, J. Silva-Leon, J. O'Connor, and A. Revell, "An experimental and computational study on inverted flag dynamics for simultaneous wind-solar energy harvesting", *Fluids*, vol. 4, no. 2, 2019, ISSN 2311-5521, doi:10.3390/fluids4020087.
- [22] J. Silva-Leon, A. Cioncolini, M. Nabawy, A. Revell, and A. Kennaugh, "Simultaneous wind and solar energy harvesting with inverted flags", *Applied Energy*, vol. 239, pp. 846–858, 2019, ISSN 0306-2619, doi:10.1016/j.apenergy.2019.01.246.
- [23] L. Jiang, Y. Yang, R. Chen, G. Lu, R. Li, D. Li, M. Humayun, K. Shung, J. Zhu, Y. Chen, and Q. Zhou, "Flexible piezoelectric ultrasonic energy harvester array for bio-implantable wireless generator", *Nano Energy*, vol. 56, pp. 216–224, 2019, ISSN 2211-2855, doi:10.1016/j.nanoen.2018.11.052.
- [24] R. Song, C. Hou, C. Yang, X. Yang, Q. Guo, and X. Shan, "Modeling, validation, and performance of two tandem cylinder piezoelectric energy harvesters in water flow", *Micromachines*, vol. 12, no. 8, 2021, ISSN 2072-666X, doi:10.3390/mi12080872.
- [25] F. Martínez, F. Martinez, and H. Ariza, "Low cost, high performance fuel cell energy conditioning system controlled by neural network", *TELKOMNIKA (Telecommunication Computing Electronics and Control)*, vol. 18, p. 3116, 2020, doi:10.12928/telkomnika.v18i6.16426.
- [26] F. Martínez, C. Penagos, and L. Pacheco, "Scheme for motion estimation based on adaptive fuzzy neural network", *TELKOMNIKA (Telecommunication Computing Electronics and Control)*, vol. 18, p. 1030, 2020, doi:10.12928/telkomnika.v18i2.14752.
- [27] E. Caicedo, C. Bautista, and A. Grisales, "Nanotechnology in the construction industry", *Tekhnê*, vol. 16, no. 2, pp. 13–20, 2019, ISSN 1692-8407.